Astron. & Astrophys. 43, 459—463 (1975)

Research Note

A High Resolution Map of the Supernova Remnant 3C 400.2 at 610 MHz

W. M. Goss
Kapteyn Astronomical Institute and Raman Research Institute

S. G. Siddesh
Raman Research Institute

U. J. Schwarz
Kapteyn Astronomical Institute

Received June 24, 1975

Summary. The large supernova remnant 3C 400.2 has been mapped with the Westerbork synthesis telescope at 610 MHz (49 cm) with a resolution of $1' \times 3'$. The linear relative resolution is roughly a factor of 20. The shell structure is quite clearly visible. A comparison with an 11 cm map made by Willis (1973) shows that the spectral index between 49 and 11 cm is constant over most of the source. The spectral index does however steepen in the central depression. A shell model has been fitted to the observations and the faint filaments found by van den Bergh *et al.* (1973) can be identified with a secondary maximum in the SNR.

Key words: supernova remnant

Introduction and Observations

Holden and Caswell (1969) have pointed out that the extended 3C source (3C 400.2, G53.6–2.2) is probably a supernova remnant due to its low galactic latitude and high brightness temperature at 178 MHz. Subsequent observations at 11 cm by Day *et al.* (1972), Willis (1973) and Velusamy and Kundu (1974) have shown a partial shell structure characteristic of many galactic SNR. The highest resolution employed by the latter two groups was $\sim 5'$ while the SNR is $\sim 30'$ in size. Willis has applied the observed surface brightness-source diameter method ($\Sigma - d$) to 3C 400.2 and derived a linear diameter of ~ 40 pc and a distance of ~ 4 kpc. The size and surface brightness are thus similar to the Cygnus Loop, another old evolved SNR.

In order to further the study of this large supernova, we have mapped it at 610 MHz using the Westerbork Synthesis Radio Telescope. The observations were carried out in autumn 1973 during a 2×12^h period with 40 interferometers. The shortest spacing is 36 m and the longest is 1440 m with an increment of 36 m. The resultant first grating ring has a radius of $46'$ in right ascension and hence is well outside the source. The grating responses from background sources can however interfere with the source. In order to approach the theoretical sensitivity expected, it was necessary to subtract 15 sources with grating response from the map. As an example the 4C source (4C 16.55) gives rise to a grating ring which runs through the SNR. After the 15 sources were subtracted the rms noise measured outside the source is 4 m.f.u.[1])/beam or 1.3 K brightness temperature. The synthesized HPBW is $50'' \times 187''$. The source list is given in Table 1; the fluxes have been corrected for the primary beam attenuation. For 4C 16.65 the spectral index, $\alpha (S \alpha \nu^{\alpha})$, is -0.7 ± 0.1 between 178 and 610 MHz.

SNR 3C 400.2

In Fig. 1 we present the full resolution ($60'' \times 187''$) map at 610 MHz. Two point sources (Nos. 4 and 6 in Table 1) have been subtracted in this contour map and the positions are indicated by crosses. The other background sources lie outside the area shown in Fig. 1. In previous lower resolution maps various contributions of these two sources are included in the emission attributed to the SNR. We assume that these two are random background sources and are probably of an extragalactic origin. Both sources are quite comparable in intensity to other background sources in the field. In this respect we agree fully with the conclusions of

[1]) 1 m.f.u. (milli flux unit) $= 10^{-29}$ W m^{-2} Hz^{-1}.

Table 1. Source list

Source no.	Position (1950)		Flux density (m.f.u.)	Remarks
	R.A. h m s s	Dec. ° ′ ″ ″		
1	19 32 35.7±0.3	17 25 37±11	900±100	(1060 m.f.u. at 408 MHz)[a])
2	19 33 30.0±0.2	16 42 07± 9	1400±125	4C 16.65 (1860 m.f.u. at 408 MHz)[a])
3a	19 35 20.2±1.0	16 43 34±44	45± 20	Apparent double source
3b	19 35 25.7±0.3	16 41 32±14	80± 20	
4	19 35 25.0±0.3	17 18 45±13	380± 50	
5	19 35 50.8±0.2	17 52 22±10	110± 10	
6	19 36 18.1±0.3	17 30 52±14	320± 50	
7	19 36 44.0±0.5	17 46 23±16	165± 30	
8a	19 37 52.2±1.0	16 49 2±35	45± 20	Apparent double source
8b	19 38 1.8±2.0	16 49 6±53	20± 15	
9	19 38 22.0±0.3	16 25 4± 8	130± 20	
10	19 38 35.8±0.5	17 04 3±25	125± 40	
11	19 39 29.0±0.2	17 29 54±10	160± 20	
12	19 40 27.0±1.0	17 01 17±35	100± 10	
13	19 40 46.8±0.3	16 33 18±10	400± 60	

[a]) Clark and Crawford, 1974.

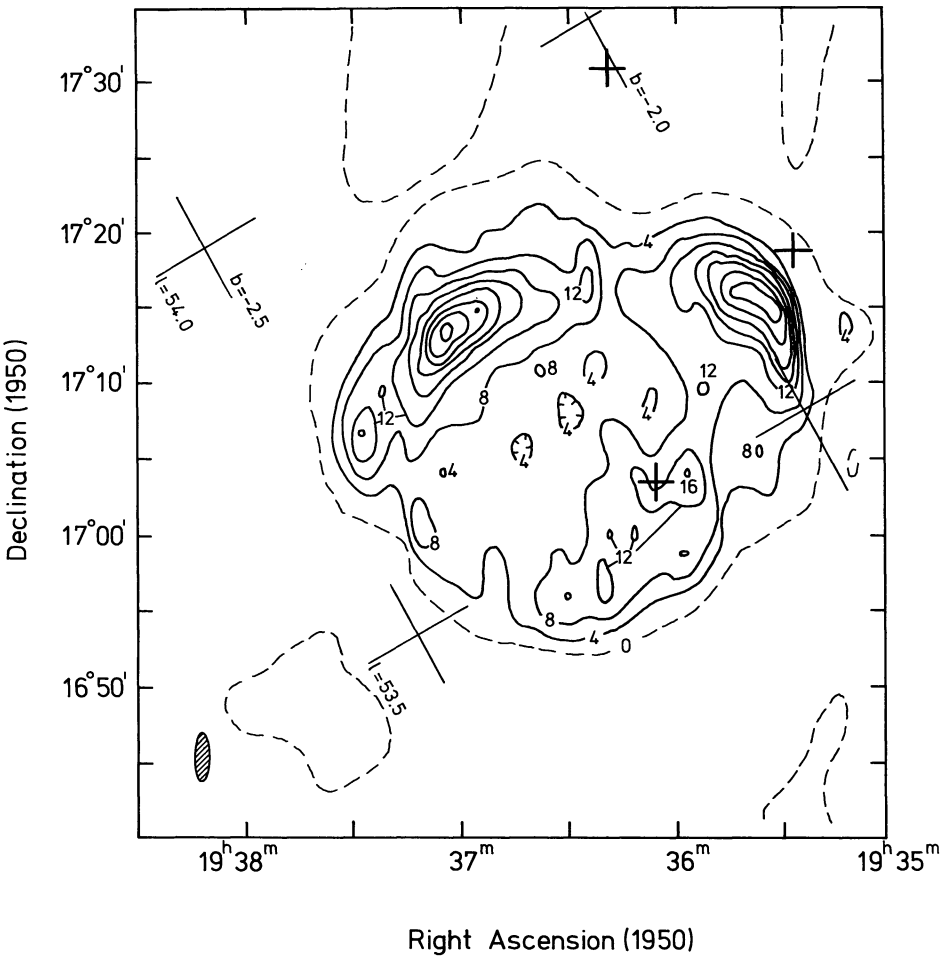

Fig. 1. Full resolution contour map at 610 MHz. The contours are labelled in units of 5 m.f.u./beam or 1.6 K in brightness temperature. The zero level contour is dotted. To correct for the missing zerospacing 2.5 K must be added to all temperatures. The upper two crosses correspond in positions to sources 6 and 4 (listed in Table 1), respectively, starting from the top of the figure. These two sources have been subtracted in the map. The lower cross gives the position of the bright optical filament observed by van den Bergh *et al.* (1973)

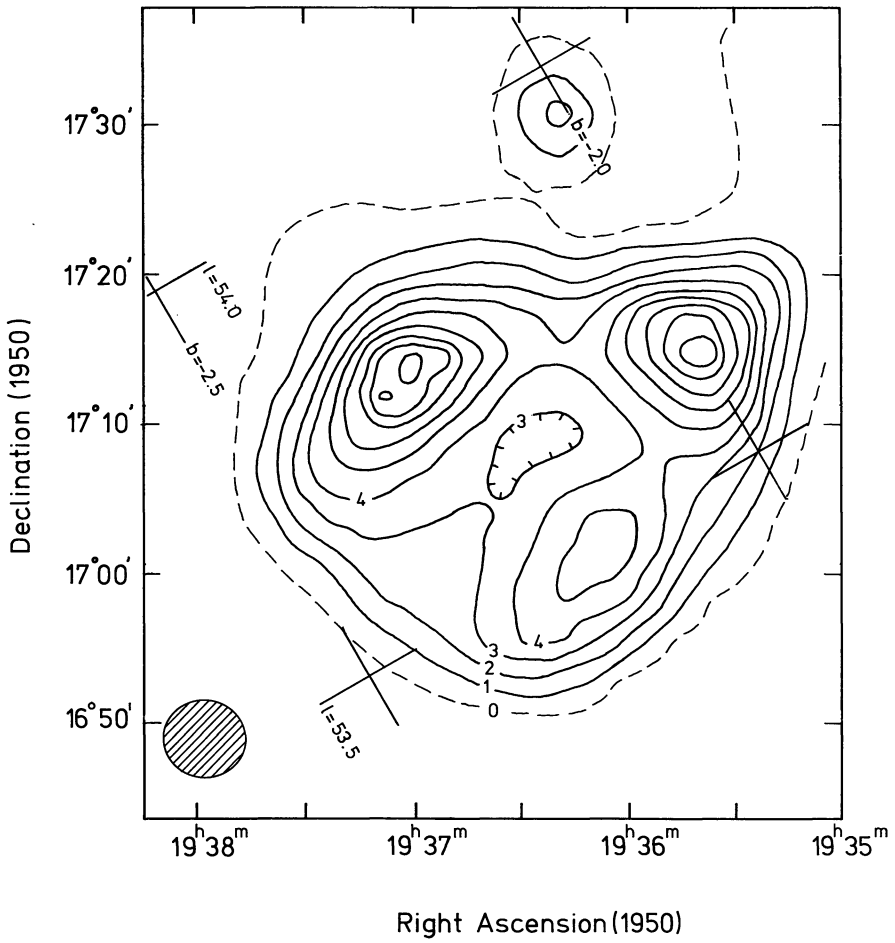

Fig. 2. 610 MHz contour map smoothed to a HPBW of 5'.1 × 5'.4. Sources 4 and 6 listed in Table 1 have been included in this map. The contour interval is 98 m.f.u./beam or 3.5 K in brightness temperature. The zero level contour is dotted. To correct for the missing zerospacing 2.5 K must be added to all temperatures

Willis (1973) about the background nature of most of the point sources near galactic SNR.

The total flux at 49 cm in Fig. 1 is 13.2±1.6 f.u. (after correction for the missing zerospacing), which is in good agreement with the 610.5 MHz flux measured by Wendker and Yang (1968) of 12±2.4 f.u. The source shows a well developed shell structure with major peaks to the north-east (54 K) and to the north-west (47 K). The latter is unresolved at the very steep edge to the west. The central depression shows an average brightness temperature of 11 K.

In Fig. 2 we show a smoothed 49 cm map with a HPBW of 5'.1 × 5'.4. This map was produced from the data in Fig. 1 by convolution and has a comparable resolution to the 11 cm map presented by Willis (1973) of 4'.9 × 5'.7. Sources Nos. 4 and 6 have been included as they have not been subtracted in the 11 cm map. This explains the extension in the north-west corner. We have made a detailed comparison of our 49 cm map with the 11 cm map. Over much of the source the brightness temperature spectral index has a constant value of −2.60±0.05 which is expected from the flux spectral index of −0.62±0.04 given by Willis (1973). However, near the central hole where the 49 cm brightness temperature is ~13 K there is a steepening of the spectral index to −2.8±0.05.

In Fig. 3 we show radial profiles of surface brightness at 11 and 49 cm; the 11 cm data is taken directly from Willis (1973) and the 49 cm data has been produced from the map in Fig. 2. Profiles were produced by averaging concentric annuli spaced by 2'.5. The data at both frequencies are normalized to unity at the peak where the brightness spectral index is −2.6. The increase in the spectral index towards the central region is obvious. The lack of agreement of the two curves at a radius of ~18' is probably due to source No. 4 which may have a spectral index slightly steeper than the SNR.

Shell Model

We have attempted to determine the properties of the shell distribution giving rise to 3C 400.2 by two different methods. For both methods spherical symmetry and optical thinness are assumed. In addition we assume

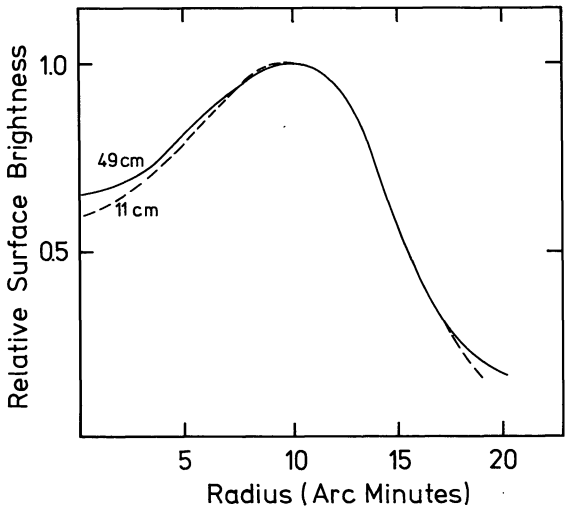

Fig. 3. The radial distribution of surface brightness at $\lambda = 49$ cm and $\lambda = 11$ cm. The 49 cm profile is produced from Fig. 2. The centre of the source is R.A. (1950) = $19^h36^m26^s$ and Dec. (1950) = 17°68′14″. The 11 cm data (dashed) is taken from Willis (1973). At the peak, where the relative surface brightness is normalized to unity, the brightness spectral index is −2.6

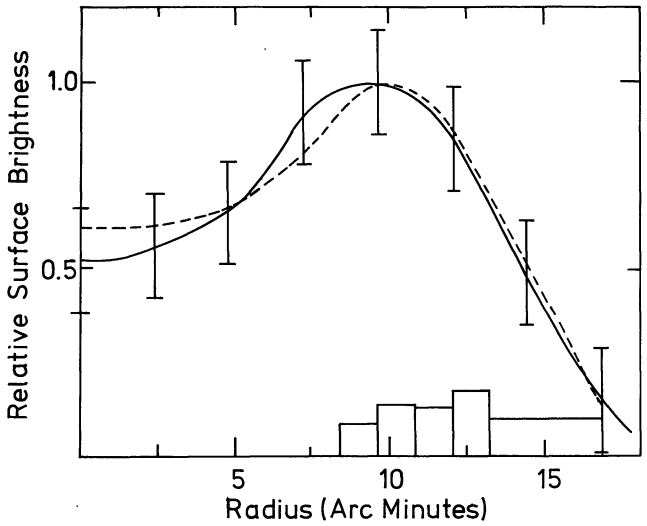

Fig. 4. The solid line represents the mean observed radial distribution of surface brightness derived from Fig. 1 with annuli spaced by 2′.4. The σ(rms) of the brightness distribution for each of the annuli is also shown as vertical bars. The source centre is at R.A. (1950) = $19^h36^m25^s$ and Dec. (1950) = 17°09′00″ and the average is produced over sectors from 0 to 360°. At the peak, where the relative surface brightness has been normalised to unity, the brightness temperature is 20.1 K. The distribution of volume emissivity computed from the method suggested by Hill (1967) is shown in histogram form and is in the same units following Hill. The slight differences between various shells are not significant. The radial brightness distribution computed from the model is shown by a dashed line

isotropic emission. For Cas A (Rosenberg, 1970) and Tycho (Strom and Duin, 1973) it is necessary to include a non-isotropic component produced by a magnetic field with a radial orientation. For these sources this assumption is quite justified in view of the radial nature of the observed magnetic field. For 3C 400.2 the polarization observations at 11 cm are uncertain. Willis (1973) with a 5′ HPBW and Caswell and Goss (unpublished data) with a 8′ HPBW find that any polarization attributable to 3C 400.2 is masked by the polarization of the galactic background. Velusamy and Kundu (1974) with a 5′ HPBW find marginal evidence for polarization in the eastern peak. Due to the unknown orientation of the magnetic field we can only assume that the emission is isotropic.

The first method attempted was that of fitting shells, each with uniform emission following a method derived by Hill (1967). This shell model is shown in Fig. 4; each shell has a thickness of 1′.2 since the radial profile was constructed with annuli spaced by 2′.4. Within the errors of the fit the slight differences in emissivity between the various shells are not significant. The outer radius of 17′ and the thickness of 8′ are in excellent agreement with the values obtained by Willis at 11 cm with slightly poorer resolution. The poorer fit at the centre [found also by Willis (1973)] is due either to (i) slight beaming due to a radial magnetic field or (ii) deviations from spherical symmetry. Since such deviations are quite pronounced, (ii) is the most likely cause. To illustrate the large observed departure from circular symmetry, the σ(rms) of the distribution of brightness in each of the annuli is also plotted in Fig. 4.

The second method of determining the properties of the shell was to solve the Abel integral equation relating the volume emissivity and the observed radial distribution of brightness as given in Fig. 4. The resulting emissivity is in good agreement with the shell model shown in Fig. 4. The mean radius of the shell is 11′.8 and the width to halfpower is 7′.5.

Optical Emission

Van den Bergh *et al.* (1973) have called attention to weak optical filaments which can be associated with 3C 400.2. Reference to his Fig. 20 shows filaments extending over ∼7′ with position angle of ∼130°. The two brightest stars in their Fig. 20 are BD 16° 3928 (∼$7^m.5$) and to the south BD 16° 3925 (∼$6^m.9$). The brightest filamentary patch is at R.A. (1950) = $19^h36^m06^s$, Dec. (1950) = 17°03′.5 which coincides with a local maximum in the radio maps. This position is marked in Fig. 1. The curvature in optical filaments corresponds to the shape of the radio source as shown by contour 8 in the southwest region. Reference to the Palomar Sky Atlas blue and red plates indicates that the extinction increases rapidly to the north of the SNR. The dark nebulae are L729, L731 and L737 (Lynds, 1962); these objects have opacities of classes 4 and 5. This variable extinction probably accounts for the weakness of the optical emission and the absence of filaments from the two maximum in the SNR. It may well be that 3C 400.2

shows the good correlation between filaments and radio structure found in other old SNR as discussed by Duin (1974) and Hill (1972) for IC 443 and by Moffat (1971) for the Cygnus Loop.

Discussion

The spectral index increase to the centre between 11 and 49 cm is very similar to the case of Tycho (3C 10) between 21 and 49 cm found by Duin (1974). Duin has made the plausible suggestion that this steepening of the spectrum towards the centre of Tycho is due to an increase of shell thickness towards lower frequencies. In this model the relativistic electrons that are accelerated near the shock have a flatter spectrum as compared to the original electron spectrum which is closer to the source of the explosion. However the applicability of this model to 3C 400.2 is questionable due to the extreme differences in age. From the similarities in surface brightness of the Cygnus Loop and 3C 400.2 the age of the latter SNR must be $\geqq 10^4$ years while that of Tycho is 400 years. From these differences it appears likely that 3C 400.2 is in Phase III (momentum conserving stage; Woltjer, 1970) while it is generally accepted that Tycho is in Phase II (the adiabatic or blast wave phase).

A similar problem concerns the nature of the thick shell (which does *not* arise from resolution effects) of 3C 400.2. In many treatments of the $\Sigma - d$ relation, the shell thickness (ΔR) remains constant as the shell radius R evolves. However observational evidence (Shaver and Goss, 1970; Willis, 1973) suggests that $\Delta R/R$ is more or less constant as a function of radius. Dynamical models also predict a thin shell (see e.g. Rosenberg and Scheuer, 1973). 3C 400.2 is a good example of a thick shell SNR ($\Delta R/R \sim 0.5$) that is quite evolved. (Many of the younger SNR have $\Delta R/R \sim$ 0.2–0.3.) In this respect 3C 400.2 is different from the Cygnus Loop for which $\Delta R/R$ is ~ 0.05. The causes of this difference undoubtedly lie in the details of the past evolution of the SNR. Another example of a thick shell of an evolved SNR is HB21 (Hill, 1974).

One of the most striking properties of 3C 400.2 (Figs. 1 and 4) is the asymmetrical distribution of emission which is a characteristic feature of most of the low-brightness evolved SNR (e.g. Cygnus Loop, IC 443, HB9, HB21 and CTB1). The two pronounced peaks to the northeast and northwest account for 20–30% of the flux at 49 cm. Both the age of the SNR plus this assymetry indicate that the present state of evolution is governed strongly by the interaction with the surrounding interstellar medium. It is noteworthy that the two areas of enhanced emission are on the side of the SNR closest to the galactic plane. (There is no information about the distances of the dark nebulae to the north; they are probably at distances <1 kpc and hence have no relation to the SNR surrounding.) Since the outer boundary of the source is still quite circular (to within $\sim 20\%$) this implies that the interaction with the interstellar medium must have occurred in the recent past. Irregularities in radius are only weakly dependent on the surrounding density for Phase III ($R \propto \varrho^{-1/4}$) whereas the synchrotron emission enhancement is proportional to a much higher power of the density since both the magnetic field and relativistic particle density increase at the shock. For 3C 400.2 the increased emission is quite evident without the obvious deviations from circularity that are observed in the Cygnus Loop, IC 443, CTB 1 and OA 184 (Willis, 1973).

Acknowledgements. The Westerbork Synthesis Radio Telescope is operated by the Netherlands Foundation for Radio Astronomy with the financial support of the Netherlands Organization for the Advancement of Pure Research (Z.W.O.). Goss acknowledges support from Z.W.O. and thanks Prof. V. Radhakrishnan for his hospitality at the Raman Research Institute in Bangalore. We thank M.K.V. Bappu for assistance with the optical identification and V. Radhakrishnan, A.G. Willis and J.L. Caswell for helpful comments.

References

Bergh, S. van den, Marscher, A.P., Terzian, Y. 1973, *Astrophys. J. Suppl.* **26**, 19
Clark, D.H., Crawford, D.F. 1974, *Australian J. Phys.* **27**, 713
Day, G.A., Caswell, J.L., Cooke, D.J. 1972, *Australian J. Phys. Astrophys. Suppl.* **25**, 1
Duin, R.M. 1974, Ph.D. thesis, Leiden University
Hill, E.R. 1967, *Australian J. Phys.* **20**, 297
Hill, I.E. 1972, *Monthly Notices Roy. Astron. Soc.* **157**, 419
Hill, I.E. 1974, *Monthly Notices Roy. Astron. Soc.* **169**, 59
Holden, D.J., Caswell, J.L. 1969, *Monthly Notices Roy. Astron. Soc.* **143**, 407
Lynds, B.J. 1962, *Astrophys. J. Suppl.* **7**, I
Moffat, P.H. 1971, *Monthly Notices Roy. Astron. Soc.* **153**, 401
Rosenberg, I. 1970, *Monthly Notices Roy. Astron. Soc.* **151**, 109
Rosenberg, I., Scheuer, P.A.G. 1973, *Monthly Notices Roy. Astron. Soc.* **161**, 27
Shaver, P.A., Goss, W.M. 1970, *Australian J. Phys. Astrophys. Suppl.* **14**, 133
Strom, R.G., Duin, R.M. 1973, *Astron. & Astrophys.* **25**, 351
Velusamy, T., Kundu, M.R. 1974, *Astron. & Astrophys.* **32**, 375
Wendker, H., Yang, K.S. 1968, *Astron. J.* **78**, 61
Woltjer, L. 1970, I.A.U. *Symp.* **39**, 229
Willis, A.G. 1973, *Astron. & Astrophys.* **26**, 237

W.M. Goss
CSIRO, Division of Radiophysics
P.O. Box 76
Epping, N.S.W., 2121, Australia

S.G. Siddesh
Raman Research Institute
Hebbal P.O.
Bangalore-560006, India

U.J. Schwarz
Kapteyn Astronomical Institute
P.O. Box 800
Groningen, The Netherlands